International Journal of Fluid Mechanics Research, Vol. 26, Nos. 5 & 6, 1999

Oscillatory Natural Convection Flow of a Two-Phase Suspension over a Surface in the Presence of Magnetic Field and Heat Generation Effects

A. J. Chamkha and **J. A. Adeeb**
Department of Mechanical and Industrial Engineering, Kuwait University
Safat, Kuwait

A continuous two-phase flow and heat transfer model is derived taking into account natural convection currents and is applied to the problem of laminar, hydromagnetic, oscillatory flow of a Newtonian, electrically-conducting, and heat generating or absorbing fluid with solid, monodispersed spherical suspended particles over a vertical infinite surface. The surface is assumed permeable so as to allow for possible wall fluid- and particle-phase suction or blowing and is maintained at a constant temperature. A uniform magnetic field is applied in the direction normal to that of the flow. The free stream velocity oscillates about a constant mean value. The solid particles and the vertical surface are assumed to be electrically non-conducting and the particle-phase density distribution is assumed to be uniform. In addition, the particle-phase is assumed to have an analog pressure and is endowed by a viscosity. Furthermore, the fluid phase is assumed to have temperature-dependent heat generation or absorption effects. In the absence of viscous dissipations of both phases, Joule heating, drag-type work, and the Hall effect of magnetohydrodynamics, the derived governing equations are solved analytically for the velocity and temperature profiles of both phases using the regular perturbation technique. The analytical results are compared with previously published work and are found to be in excellent agreement. The effects of the Grashof number, Hartmann number, particle loading, Prandtl number, heat generation or absorption coefficient, viscosity ratio, and the particulate wall slip on the velocity and temperature fields of both phases are illustrated graphically to show interesting features of the solutions.

* * *

Introduction

In recent years, there has been a renewed exploration for new ideas harnessing various conventional energy sources like tidal waves, wind power, geothermal energy, nuclear reactor and many others (Hiremath and Patil [1]). It is known that for optimizing the use of geothermal energy, it is necessary to have a precise knowledge of the perturbations needed to generate convection currents

ISSN1064-2285

in geothermal fluids. Contamination of these fluids with solid particles has the tendency to affect the heat transfer characteristics of these fluids and, therefore, the use of the geothermal energy. In certain processes, these solid particles can be placed in the system deliberately or naturally. The analysis of the flow and heat transfer aspects of a two-phase particulate suspension requires the consideration of the balance laws of mass, linear momentum, and energy equations of both the fluid and particle phases. Assuming both phases as interacting continua, these equations will be coupled through interphase drag and heat transfer.

The geothermal fluids are electrically conducting and are affected by the presence of a magnetic field (Aldoss et al. [2]). Also, electrically-conducting fluids in the presence of a magnetic field are often used for the purpose of cooling of nuclear reactors and suppression of convective currents in the semi-conductor industry. Other possible applications of hydromagnetic flows are heat exchangers, magnetohydrodynamic (MHD) generators, cooling and quality control of many metallurgical processes such as drawing of continuous filaments through electrically-conducting fluids, and annealing and tinning of copper wires and others. In addition, certain situations may involve heat generation or absorption aspects such as those dealing with fluids undergoing exothermic or endothermic chemical reactions (Vajravelu and Hadjinicolaou [3]). The presence of these characteristics for the carrier fluid along with the effect of particle loading in a fluid-particle suspension can alter the flow and heat transfer features significantly. Therefore, the purpose of this work is to consider unsteady, laminar, hydromagnetic, oscillatory fluid-particle flow over a vertical, permeable, infinitely long plate in the presence of fluid buoyancy and heat generation or absorption effects.

Chamkha and Ramadan [4] have reported steady state analytical solutions for laminar free convection two-phase (fluid-particle) flow over a vertical infinite permeable plate. They have shown that the presence of particles in the carrier fluid causes significant changes in the flow and heat transfer characteristics.

Raptis and Perdikis [5] have studied oscillatory flow of a Newtonian fluid through a porous medium in the presence of free convection currents. Also, Hiremath and Patil [1] have considered free convection effects on the oscillatory flow of a couple stress fluid through a porous medium and have reported some results for the case of a Newtonian fluid. Since the presence of a magnetic field results in a linear drag-like resistive force in the momentum equation as in the case of flow in a Darcian porous medium, then the results of Raptis and Perdikis [5] and Hiremath and Patil [1] can be used for comparison as a limiting case of the general problem of this work when the particle loading and heat generation or absorption effects are omitted from the model.

The following referenced work can not be used for comparison but they represent some of the work done on oscillatory flow and their application. Levesley and Bellhouse [6] have reported on the retention and suspension of particles in a fluid using oscillatory flow within a straight channel. The degree of retention of particles was experimentally correlated with the frequency and amplitude of the applied oscillation. Smith [7] has analyzed slow oscillatory Stokes flow. Hall et al. [8] have compared oscillatory and stationary flow through porous media. The empirical coefficients determined from steady stationary flow were generally found to apply to the unsteady flow situation with some dependence on the period of oscillations. Foote et al. [9] have reported some exact solutions of the Stokes problem for an elastico-viscous fluid using the Taylor series expansion which compared with the pertubation solutions obtained in some earlier investigations. The problem of oscillatory flow in a stratified medium past an infinite porous plate with constant suction was considered by Soundalgekar and Shende [10]. Duck and Bodonyi [11] have analyzed oscillatory flow over a semi-infinite plate at low Reynolds numbers. Mazumdar and Das [12] studied dispersion of contaminants in oscillatory flow through a pipe. The purpose of this work is to consider

oscillatory two-phase (fluid-particle) natural convection flow over an infinite permeable vertical plate or surface in the presence of magnetic field and heat generation or absorption effects.

Problem Formulation

Consider unsteady, laminar two-dimensional natural convection flow of a two-phase particulate suspension over an infinitely long vertical permeable surface in the presence of a transverse magnetic field. Uniform fluid-phase suction (or injection) is imposed at the surface which is maintained at a uniform temperature T_w. Far from the surface, the suspension (fluid plus particles) oscillates about a mean value with direction parallel to that of the surface. The two-phase flow takes place in the xy plane with the surface being placed at $y = 0$. The x-axis is taken along the surface with the positive direction being opposite to the direction of gravity and the y-axis is taken to be normal to the surface (see Fig. 1). A magnetic field of uniform strength is applied normal to the plate or surface which affects the electrically-conducting fluid phase. However, the particle phase will be affected by the magnetic field indirectly through the drag force existing between the fluid and particle phases. The magnetic Reynolds number is assumed to be small so that the induced magnetic field is neglected. Also, no electrical field is assumed to exist and the effects of Joule heating and viscous dissipations of both phases as well as the Hall effect are assumed negligible. In addition, the fluid-phase heat generation or absorption effects are assumed to be temperature dependent. All fluid and particle-phase properties are assumed to be constant except the fluid-phase density in the buoyancy term of the x-momentum equation. Since the plate or surface is infinite, all of the dependent variables of the problem will only depend on the y-direction and time t. Assuming that the Boussinesq approximation is valid and treating the particle phase as a continuum, the governing equations for this investigation, with all of the previously-stated assumptions taken into consideration, can be written as

$$\frac{\partial v}{\partial y} = 0 \tag{1}$$

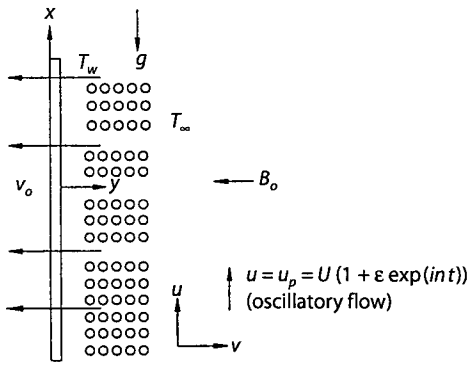

Fig. 1. Physical model and coordinate system.

$$\rho\left(\frac{\partial u}{\partial t}+v\frac{\partial u}{\partial y}\right)=-\frac{\partial P}{\partial x}+\mu\left(\frac{\partial^2 u}{\partial y^2}\right)+\rho_p N(u_p-u)-\rho g-\sigma B_o^2 u \tag{2}$$

$$\rho c\left(\frac{\partial T}{\partial t}+v\frac{\partial T}{\partial y}\right)=k\left(\frac{\partial^2 T}{\partial y^2}\right)+Q_o(T-T_\infty)+\rho_p N_T c_p(T_p-T) \tag{3}$$

$$\frac{\partial(\rho_p v_p)}{\partial y}=0 \tag{4}$$

$$\rho_p\left(\frac{\partial u_p}{\partial t}+v_p\frac{\partial u_p}{\partial y}\right)=-\frac{\partial P_p}{\partial x}+\mu_p\left(\frac{\partial^2 u}{\partial y^2}\right)+\rho_p N(u-u_p)-\rho_p g \tag{5}$$

$$\rho_p c_p\left(\frac{\partial T_p}{\partial t}+v_p\frac{\partial T_p}{\partial y}\right)=\rho_p N_T c_p(T-T_p) \tag{6}$$

where t stands for time and x and y represent distances along and normal to the surface, respectively. u, v, P, and T are the fluid-phase x-component of velocity, y-component of velocity, pressure, and temperature, respectively. ρ, μ, c, and k are the fluid-phase density, dynamic viscosity, specific heat and thermal conductivity, respectively. σ, B_o, Q_o, and g are the fluid-phase electrical conductivity, the magnetic induction, the heat generation (> 0) or absorption (< 0) coefficient, and the acceleration due to gravity, respectively. N, N_T, and T_∞ are the interphase momentum transfer coefficient, interphase heat transfer coefficient, and the free stream temperature, respectively. A subscript p denotes the same property for the particle phase. It can be clearly seen from Eqs. (2), (3), (5), and (6) that the flow and heat transfer aspects of both phases are coupled through the interphase drag and heat transfer mechanisms.

The physics of the problem suggests the following boundary conditions:

$$u(t,0)=0 \qquad v(t,0)=-v_o \qquad u_p(t,0)=0 \qquad v_p(t,0)=-v_o$$

$$\frac{\partial u_p}{\partial y}(t,0)=\omega^* u_p(t,0)$$

$$T(t,0)=T_w \qquad T(t,\infty)=T_p(t,\infty)=T_\infty$$

$$u(t,\infty)=u_p(t,\infty)=U_\infty=U^*(1+\varepsilon\exp(in^*t)) \tag{7a–h}$$

where v_0 is the suction or injection velocity, ω^* is a particle-phase wall slip coefficient, ε is a perturbation parameter, n^* is the frequency of oscillations and "i" is the complex parameter. It should be mentioned that the exact form of boundary conditions to be satisfied by the particle phase at the surface are unknown at present. However, there is some experimental evidence that a particle tends to slip at a wall. For this reason and because the motion of the particle phase which consists of discrete particles may resemble that of a rarefied gas, the form given in Eq. (7e) is employed. This type of boundary conditions is used in rarefied gas dynamics and it allows for perfect slip situations for $\omega^* = 0$, for no-slip situations for $\omega^* = \infty$, and for moderate slip situation for finite values of ω^*.

In addition, it can be seen from Eqs. (7g) and (7h) that both the fluid and the particle phases are in both hydrodynamic and thermal equilibrium.

Evaluating Eqs. (2) and (5) at the free stream conditions ($y = \infty$) gives:

$$\rho\left(\frac{dU_\infty}{dt}\right) = -\frac{\partial P}{\partial x} - \rho_\infty g - \sigma B_o^2 U_\infty \tag{8}$$

$$\rho_p\left(\frac{dU_\infty}{dt}\right) = -\frac{\partial P_p}{\partial x} - \rho_p g \tag{9}$$

where ρ_p is the free-stream density for the fluid phase. By eliminating the pressure gradients from Eqs. (2) and (8) as well as from (5) and (9) yields

$$\rho\left(\frac{\partial u}{\partial t} + v\frac{\partial u}{\partial y}\right) = \rho\frac{dU_\infty}{dt} + (\rho_\infty - \rho)g + \sigma B_o^2 (U_\infty - u) + \mu\frac{\partial^2 u}{\partial y^2} + \rho_p N(u_p - u) \tag{10}$$

$$\rho_p\left(\frac{\partial u_p}{\partial t} + v_p\frac{\partial u_p}{\partial y}\right) = \rho_p\frac{dU_\infty}{dt} + \mu_p\frac{\partial^2 u_p}{\partial y^2} + \rho_p N(u - u_p) \tag{11}$$

Applying the Boussinesq approximation

$$\rho_\infty - \rho = \rho\beta_o (T - T_\infty) \tag{12}$$

(where β_0 is the thermal expansion coefficient) in Eq. (10) reduces it to

$$\rho\left(\frac{\partial u}{\partial t} + v\frac{\partial u}{\partial y}\right) = \rho\frac{dU_\infty}{dt} + \rho\beta_o (T - T_\infty) + \sigma B_o^2 (U_\infty - u) + \mu\frac{\partial^2 u}{\partial y^2} + \rho_p N(u_p - u) \tag{13}$$

Thus, the governing equations for this problem include Eqs. (1), (3), (4), (6), (11), and (13).

With the particle-phase density ρ_p being constant, Eqs. (1) and (4) are integrated subject to the boundary conditions for v and v_p to give

$$v = v_p = -v_o \tag{14}$$

It should be mentioned that the y-momentum equations which are not written here for brevity require that v and v_p be equal. In this way both of these equations will be identically satisfied.

It is convenient to use the following parameters

$$\eta = \frac{yv_o}{\nu} \qquad \tau = \frac{tv_o^2}{\nu} \qquad F = \frac{u}{U^*} \qquad U = \frac{U_\infty}{U^*}$$

$$\theta = \frac{T - T_\infty}{T_w - T_\infty} \qquad \theta_p = \frac{T_p - T_\infty}{T_w - T_\infty} \qquad F_p = \frac{u_p}{U^*} \qquad n = \frac{n^*\nu}{v_o^2} \tag{15}$$

to non-dimensionalize the governing equations and boundary conditions. Doing this yields

$$\frac{\partial F}{\partial \tau} - \frac{\partial F}{\partial \eta} = \frac{dU}{d\tau} + \mathrm{Gr}\,\theta + M^2 (U - F) + \frac{\partial^2 F}{\partial \eta^2} + K\alpha(F_p - F) \tag{16}$$

$$\frac{\partial \theta}{\partial \tau} - \frac{\partial \theta}{\partial \eta} = \frac{1}{\mathrm{Pr}} \frac{\partial^2 \theta}{\partial \eta^2} + \phi\theta + K\alpha_T \gamma(\theta_p - \theta) \tag{17}$$

$$\frac{\partial F_p}{\partial \tau} - \frac{\partial F_p}{\partial \eta} = \frac{dU}{d\tau} + \beta \frac{\partial^2 F_p}{\partial \eta^2} + \alpha(F - F_p) \tag{18}$$

$$\frac{\partial \theta_p}{\partial \tau} - \frac{\partial \theta_p}{\partial \eta} = \alpha_T (\theta - \theta_p) \tag{19}$$

$$F(\tau, 0) = 0 \qquad \frac{\partial F_p}{\partial \eta}(\tau, 0) = \omega F_p(\tau, 0) \qquad \theta(\tau, 0) = 1 \tag{20}$$

$$F(\tau, \infty) = F_p(\tau, \infty) = 1 + \varepsilon \exp(in\tau) \qquad \theta(\tau, \infty) = \theta_p(\tau, \infty) = 0 \tag{21}$$

where

$$\mathrm{Gr} = \frac{\beta_o \nu g (T_w - T_\infty)}{U^* \nu_o^2} \qquad M^2 = \frac{\sigma B_o^2 \nu}{\rho \nu_o^2} \qquad K = \frac{\rho_p}{\rho}$$

$$\alpha = \frac{N\nu}{\nu_o^2} \qquad \mathrm{Pr} = \frac{\mu c}{k} \qquad \phi = \frac{Q_o \nu}{\rho c \nu_o^2} \qquad \alpha_T = \frac{N_T \nu}{\nu_o^2}$$

$$\gamma = \frac{c_p}{c} \qquad \beta = \frac{\nu_p}{\nu} \qquad \omega = \frac{\omega^* \nu}{\nu_o} \qquad n = \frac{n^* \nu}{\nu_o^2}$$

are the Grashof number, square of the Hartmann number, particle loading, velocity inverse Stokes number, Prandtl number, dimensionless heat generation or absorption coefficient, temperature inverse Stokes number, ratio of specific heat, viscosity ratio, dimensionless particle-phase wall slip coefficient, and the dimensionless frequency of oscillations, respectively.

Analytical Solutions

In this section, closed-form solutions based on the perturbation method for the dimensionless governing Eqs. (16) through (19) subject to the boundary conditions (20) will be reported. The perturbation method is applied by assuming

$$F(\tau, \eta) = F_o(\eta) + \varepsilon \exp(in\tau) F_1(\eta)$$

$$F_p(\tau, \eta) = F_{po}(\eta) + \varepsilon \exp(in\tau) F_{p1}(\eta)$$

$$\theta(\tau,\eta) = \theta_o(\eta) + \varepsilon \exp(in\,\tau)\,\theta_1(\eta)$$

$$\theta_p(\tau,\eta) = \theta_{po}(\eta) + \varepsilon \exp(in\,\tau)\,\theta_{p1}(\eta) \tag{22}$$

Substituting Eqs. (22) into Eqs. (16) through (20) results in two sets of equations and boundary conditions. The first set governs the basic steady flow with subscript o and the second set governs the unsteady oscillatory flow with subscript 1. These sets of equations and boundary conditions can be written as

$$F_o'' + F_o' + K\alpha(F_{po} - F_o) - M^2(F_o - 1) + \mathrm{Gr}\theta_o = 0 \tag{23}$$

$$\frac{1}{\mathrm{Pr}}\theta_o'' + \theta_o' + K\alpha_T\gamma(\theta_{po} - \theta_o) + \phi\theta_o = 0 \tag{24}$$

$$\beta F_{po}'' + F_{po}' + \alpha(F_o - F_{po}) = 0 \tag{25}$$

$$\theta_{po}' + \alpha_T(\theta_o - \theta_{po}) = 0 \tag{26}$$

$$F_o(0) = 0 \qquad F_{po}'(0) = \omega F_{po}(0) \qquad \theta_o(0) = 1$$

$$F_o(\infty) = 1 \qquad F_{po}(\infty) = 1 \qquad \theta_o(\infty) = 0 \qquad \theta_{po}(\infty) = 0 \tag{27}$$

for the basic steady flow and heat transfer problem, and

$$F_1'' + F_1' + K\alpha(F_{p1} - F_1) - M^2(F_1 - 1) + \mathrm{Gr}\theta_1 + in(1 - F_1) = 0 \tag{28}$$

$$\frac{1}{\mathrm{Pr}}\theta_1'' + \theta_1' + K\alpha_T\gamma(\theta_{p1} - \theta_1) + \phi\theta_1 - in\,\theta_1 = 0 \tag{29}$$

$$\beta F_{p1}'' + F_{p1}' + \alpha(F_1 - F_{p1}) + in(1 - F_{p1}) = 0 \tag{30}$$

$$\theta_{p1}' + \alpha_T(\theta_1 - \theta_{p1}) - in\,\theta_{p1} = 0 \tag{31}$$

$$F_1(0) = 0 \qquad F_{p1}'(0) = \omega F_{p1}(0) \qquad \theta_1(0) = 0$$

$$F_1(\infty) = 1 \qquad F_{p1}(\infty) = 1 \qquad \theta_1(\infty) = 0 \qquad \theta_{p1}(\infty) = 0 \tag{32}$$

for the unsteady oscillatory and heat transfer problem. In Eqs. (23) through (32), a prime denotes ordinary differentiation with respect to η. It is obvious from the above two sets of equations that the solution of the basic steady flow problem is uncoupled from the solution of the unsteady oscillatory flow problem and, therefore, they can be solved separately.

The governing equations for the basic steady flow and heat transfer problem and the unsteady oscillatory flow and heat transfer problem are ordinary, linear, differential equations which lend themselves to be solved in closed form subject to the appropriate boundary conditions. For each of these problems the flow field is not only coupled by the presence of the particle phase through the drag force but also with the heat transfer problem through the fluid-phase buoyancy effects. These coupling effects make obtaining the analytical solutions more involved.

Combining Eqs. (24) and (26) yields a third-order linear homogeneous equation governing θ_{po}. Without going into detail, this can be shown to be

$$\theta'''_{po} + (\mathrm{Pr} - \alpha_T)\theta''_{po} + \mathrm{Pr}(\phi - \alpha_T - K\gamma\alpha_T)\theta'_{po} - (\mathrm{Pr}\,\phi\alpha_T)\theta_{po} = 0 \tag{33}$$

Equation (33) is solved subject to the appropriate boundary conditions given by Eqs. (27) to yield

$$\theta_{po}(\eta) = A_1 \exp(-m_1\eta) \qquad m_1 = -m_1^* \tag{34}$$

where

$$A_1 = \alpha_T/(\alpha_T + m_1)$$

and m_1^* is the negative root of the auxiliary equation

$$m^3 + (\mathrm{Pr} - \alpha_T)m^2 + \mathrm{Pr}(\phi - \alpha_T - K\gamma\alpha_T)m - \mathrm{Pr}\,\phi\alpha_T = 0 \tag{35}$$

It should be mentioned here that the physical solution for Eq. (35) is having only one negative root. More than one negative root will lead to undetermined constants. Also, three positive roots will lead to a trivial solution and the presence of a vanishing root obtains a vanishing constant in the solution when applied at $\eta = \infty$. It should be mentioned that in all the graphical results to be reported in the next section, this condition is satisfied.

The relation between θ_o and θ_{po} is given by

$$\theta_o = \theta_{po} - \frac{1}{\alpha_T}\theta'_{po} \tag{36}$$

Therefore, substituting the solution for θ_{po} (Eq. (34)) into Eq. (36) yields the solution for θ_o as follows

$$\theta_o(\eta) = \exp(-m_1\eta) \tag{37}$$

Similarly, combining the equations governing F_o and F_{po} yields a fourth-order, linear, non-homogeneous differential equation which can be shown to be

$$\beta F_{po}^{IV} + (1+\beta)F'''_{po} + [1 - \alpha - \beta(K\alpha + M^2)]\,F''_{po} - [\alpha(1+K) + M^2]F'_{po} + M^2\alpha F_{po} = \alpha M^2 + \mathrm{Gr}\alpha\theta_o \tag{38}$$

The general solution of this equation will consist of two parts, a homogeneous and a particular part. The auxiliary equation for the homogenous part of Eq. (38) is given by

$$\beta m^4 + (1+\beta)m^3 + [1-\alpha-\beta(K\alpha+ M^2)]m^2 - [\alpha(1+K)+M^2]m + M^2\alpha = 0 \tag{39}$$

A physically acceptable solution of Eq. (39) requires Eq. (39) to have two negative and two positives roots. Having roots that do not satisfy this condition will produce unrealistic solutions. Unfortunately, there is no way to show that Eq. (39) satisfy this condition for any values of the parameters involved in the equation. However, this condition was observed to be satisfied in all of the graphical results to be reported in the next section.

Let the two negative roots to be $(-m_2)$ and $(-m_3)$. The homogeneous solution for F_{po} can be shown to be

$$(F_{po})_h = A_2 \exp(-m_2\eta) + A_3 \exp(-m_3\eta) \tag{40}$$

where A_2 and A_3 are arbitrary constants to be determined by the boundary conditions. Substituting the solutions for θ_o (Eq. (37)) into Eq. (38) and solving for the particular solution for F_{po} gives

$$(F_{po})_p = 1 + A_4 \exp(-m_1\eta) \tag{41}$$

where

$$A_4 = \frac{\mathrm{Gr}\,\alpha}{\beta m_1^4 + (1+\beta)m_1^3 + [(1-\alpha)-\beta(K\alpha+M^2)]m_1^2 - [\alpha(1+K)+M^2]m_1 + M^2\alpha} \tag{42}$$

Thus, the general solution for F_{po} becomes

$$F_{po}(\eta) = 1 + A_2 \exp(-m_2\eta) + A_3 \exp(-m_3\eta) + A_4 \exp(-m_1\eta) \tag{43}$$

The arbitrary constant A_2 and A_3 are obtained by the application of the appropriate boundary conditions in Eqs. (27) to yield

$$A_2 = \frac{Y_1[\omega(A_4+1)+A_4m_1]-(\omega+m_3)(Z_1+1)}{(\omega+m_3)X_1-(\omega+m_2)Y_1} \tag{44}$$

$$A_3 = \frac{X_1[\omega(A_4+1)+A_4m_1]-(\omega+m_2)(Z_1+1)}{(\omega+m_2)Y_1-(\omega+m_3)X_1} \tag{45}$$

where

$$X_1 = 1 + \frac{m_2}{\alpha} - \frac{\beta m_2^2}{\alpha} \qquad Y_1 = 1 + \frac{m_3}{\alpha} - \frac{\beta m_3^2}{\alpha} \tag{46}$$

The solution for F_o is obtained from the solution

$$F_o = F_{po} - \frac{\beta}{\alpha} F''_{po} - \frac{1}{\alpha} F'_{po} \tag{47}$$

Taking the necessary derivatives and substituting of Eqs. (43) through (46) into Eq. (47) gives

$$F_o(\eta) = 1 + X_1 A_2 \exp(-m_2\eta) + Y_1 A_3 \exp(-m_3\eta) + Z_1 \exp(-m_1\eta) \tag{48}$$

With the solution for F_o, θ_o, F_{po}, and θ_{po} known, then the basic steady flow problem is determined. The solution for the unsteady oscillatory part can be found in a very similar fashion. Without going into detail, the solutions for θ_1, θ_{p1}, F_1, and F_{p1} can be shown to be

$$\theta_1(\eta) = \theta_{p1}(\eta) = 0 \tag{49}$$

$$F_{p1}(\eta) = 1 + A_5 \exp(-m_4\eta) + A_6 \exp(-m_5\eta) \tag{50}$$

$$F_1(\eta) = 1 + X_2 A_5 \exp(-m_4\eta) + Y_2 A_6 \exp(-m_5\eta) \tag{51}$$

where $(-m_4)$ and $(-m_5)$ are the only two negative roots of the auxiliary equation

$$\begin{aligned} &\beta m^4 + (1+\beta)m^3 - [\alpha + in - 1 + \beta(K\alpha + M^2) + in\beta]m^2 \\ &- [\alpha + 2in + K\alpha + M^2]m + in + K\alpha + (\alpha + in)(in + M^2) = 0 \end{aligned} \tag{52}$$

where

$$A_5 = \frac{\omega(Y_2 - 1) - m_5}{(\omega + m_5)X_2 - (\omega + m_4)Y_2} \tag{53}$$

$$A_6 = \frac{\omega(X_2 - 1) - m_4}{(\omega + m_4)Y_2 - (\omega + m_5)X_2} \tag{54}$$

$$X_2 = 1 + \frac{in}{\alpha} - \frac{\beta}{\alpha} m_4^2 + \frac{m_4}{\alpha} \qquad Y_2 = 1 + \frac{in}{\alpha} - \frac{\beta}{\alpha} m_5^2 + \frac{m_5}{\alpha} \tag{55}$$

With the solutions for the steady basic flow and the unsteady oscillatory flow, the solutions for $F(\tau, \eta)$, $F_p(\tau, \eta)$, $\theta(\tau, \eta)$ and $\theta_p(\tau, \eta)$ can be found from Eq. (22).

Results and Discussion

In this section, numerical evaluations of the analytical solutions reported in the previous section are performed and the results are compared with previously published work and reported graphically for various values of the parameters involved in the problem. This is done in order to

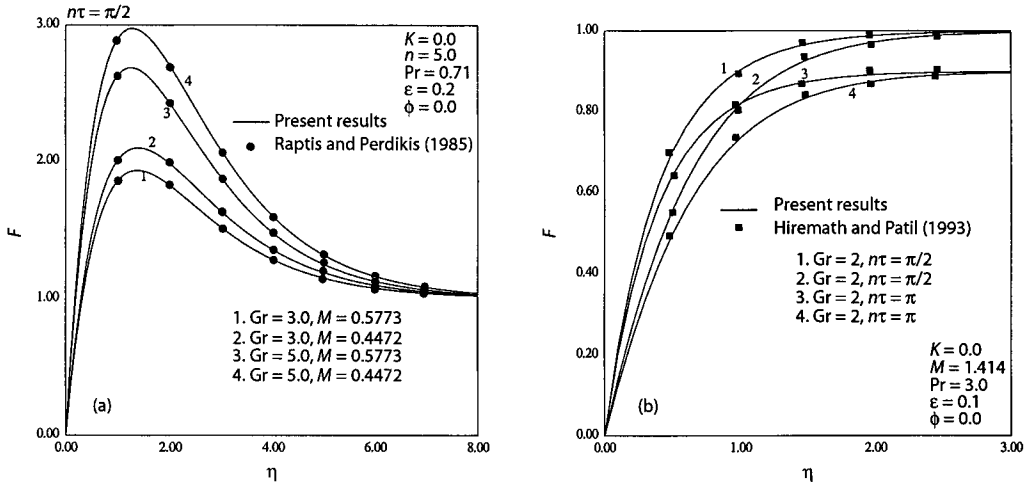

Fig. 2. (a) Comparison of velocity profile with Raptis and Perdikis (1985).
(b) Comparison of velocity profile with Hiremath and Patil (1993).

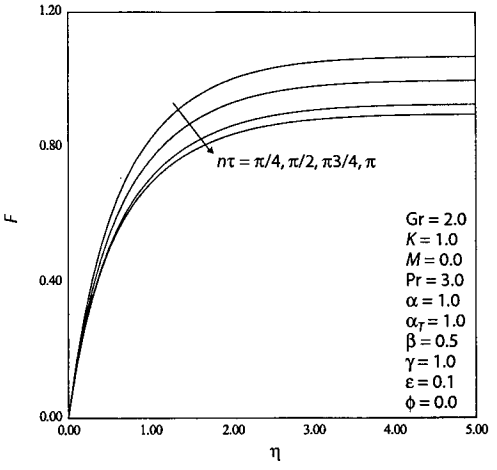

Fig. 3. Effects of $n\tau$ on fluid-phase velocity profiles.

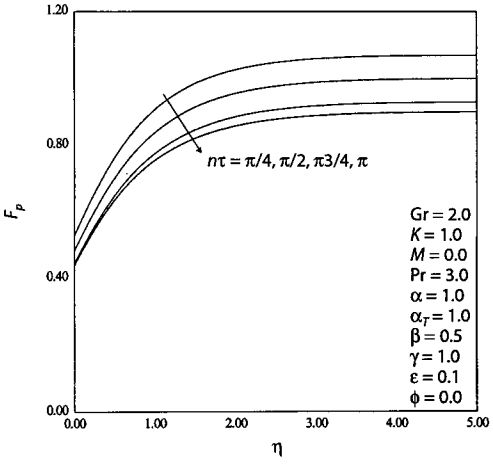

Fig. 4. Effects of $n\tau$ on particle-phase velocity profiles.

illustrate the behaviors and features of the flow and thermal problem of both the fluid and the particle phases. Figures 2 through 24 present a representative set of these results.

Figures 2a and 2b present comparisons of the fluid-phase velocity profiles for the case of a dilute suspension ($K = 0$) and in the presence of a magnetic field with those reported by Raptis and Perdikis [5] and Hiremath and Patil [1] for cooling and heating surface situations. It should be noted that the presence of the magnetic field has the same effect as that associated with a porous medium since both mechanisms cause resistance to flow. It can be clearly seen from these figures that excellent agreements between the results exist.

Figures 3 and 4 present representative profiles for the fluid-phase velocity profiles F and the particle-phase velocity profiles F_p at different $n\tau$ values, respectively. For a fixed value of τ,

increases in the frequency of oscillations n have the effect of decreasing the flow of both the fluid and particle phases at every point away from the plate surface and including the free stream conditions. The same can be said for fixing n and increasing τ. This is evident by the decreases of both F and F_p as $n\tau$ is increased in Figs. 3 and 4.

Figures 5 through 8 depict the behaviors of the fluid- and particle-phase velocity profiles (F and F_p) and the fluid- and particle-phase temperature profiles (θ and θ_p) for various values of the particle loading K for Gr = 2 which physically corresponds to cooling of the surface by free convection currents, respectively. It is seen that the presence of particles in this oscillatory flow acts as an aiding flow mechanism by which the velocities of both phases increase as the particle loading increases.

Figures 9 and 10 present typical profiles for F and F_p for various values of the magnetic parameter M, respectively. The application of the magnetic field here is observed to enhance the convec-

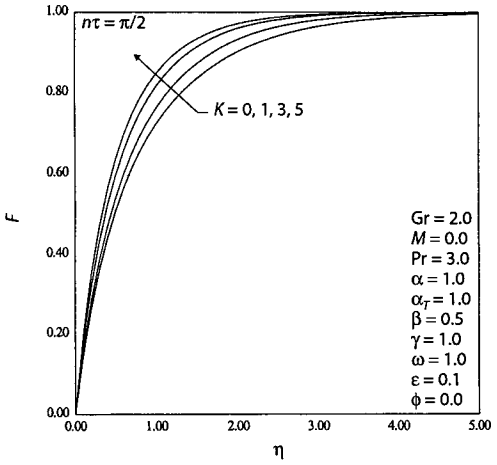

Fig. 5. Effects of K on fluid-phase velocity profiles.

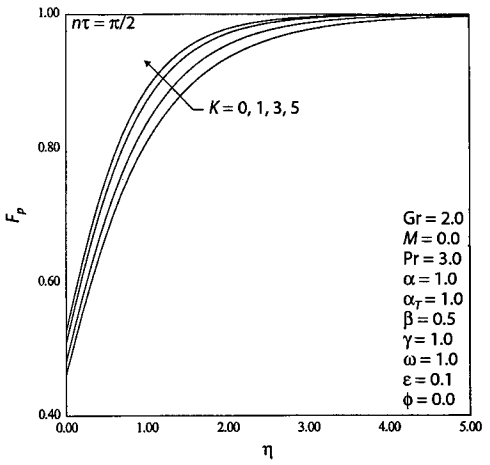

Fig. 6. Effects of K on particle-phase velocity profiles.

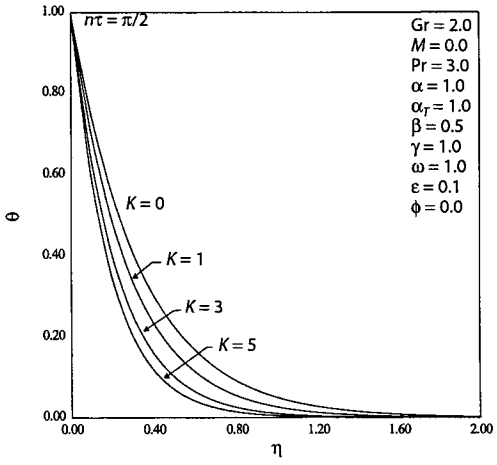

Fig. 7. Effects of K on fluid-phase temperature profiles.

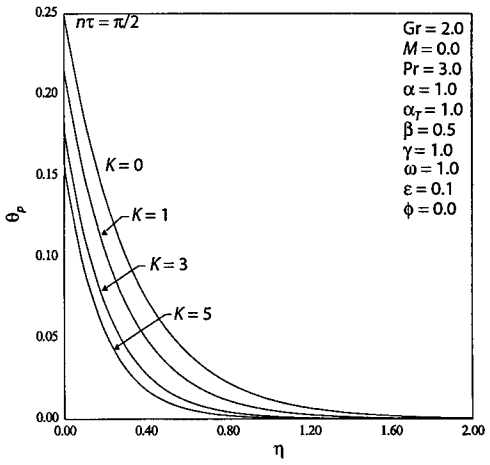

Fig. 8. Effects of K on particle-phase temperature profiles.

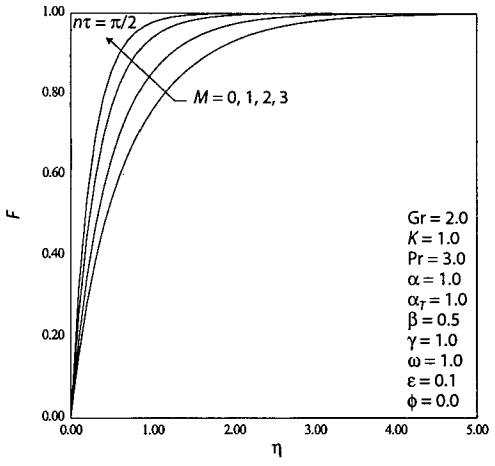

Fig. 9. Effects of M on fluid-phase velocity profiles.

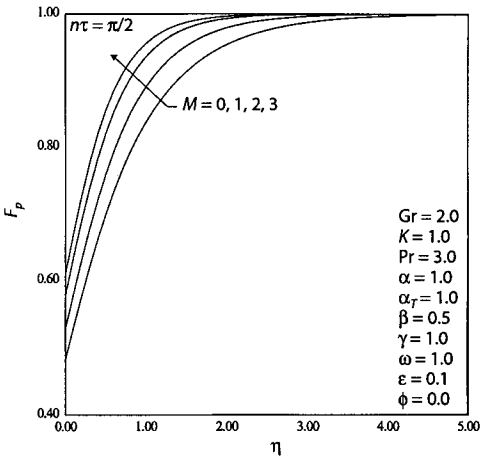

Fig. 10. Effects of M on particle-phase velocity profiles.

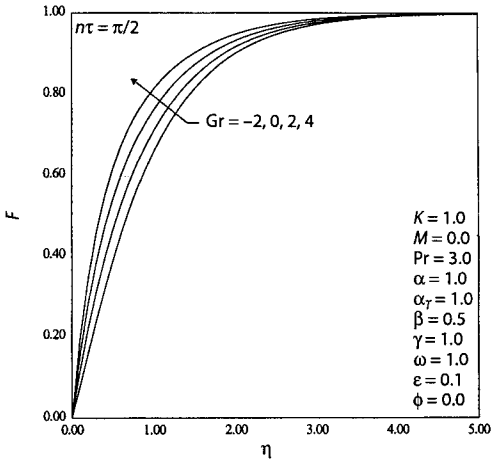

Fig.11. Effects of Gr on fluid-phase velocity profiles.

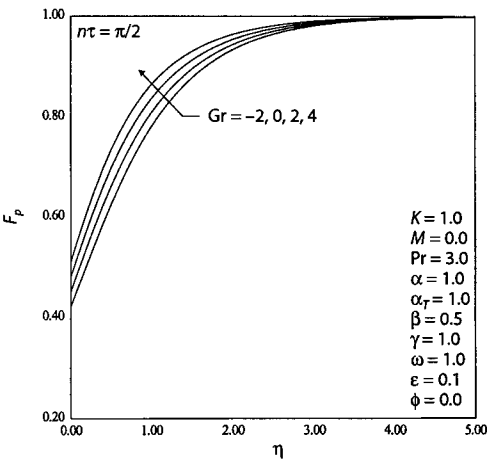

Fig.12. Effects of Gr on particle-phase velocity profiles.

tive flow along the surface. This is in contrast with other applications in which the magnetic field is used to slow down the motion of the fluid. It should be mentioned that the same effect of increased flow predicted by Hiremath and Patil (1993) by using a porous medium which has the same influence as a magnetic field.

The effects of the Grashof number Gr on the velocity profiles of both phases F and F_p are given in Figs. 11 and 12, respectively. In these figures, situations of surface heating ($Gr < 0$), surface cooling ($Gr > 0$) and non-free convection flow are illustrated. It is seen that increases in the values of Gr increase the velocities of both phases at every point from the wall. This is expected since increasing Gr increases the buoyancy effect which induces flow along the surface.

Figures 13 and 14 show the behaviors of F and F_p as the viscosity ratio β is altered, respectively. It should be noted in these figures that the particle-phase wall slip coefficient ω is set to unity

which means that the particle phase undergoes a moderate wall slip condition. This is evident from the wall velocities for the particle phase in Fig. 14. Increases in the values of β have the tendency to increase the particle-phase viscous effects. This has the effect of reducing the velocity of the particle phase. This decelerated motion in the particle phase causes the fluid phase to slow down as well. This is due to the interphase drag force existing between the phases. These behaviors are clearly illustrated in Figs. 13 and 14.

The effects of the particle-phase wall slip coefficient ω on the profiles of F and F_p are displayed in Figs. 15 and 16, respectively. It is clear from these figures that while ω has a slight decreasing effect on the profiles of F (for $K = 1$), it has a significant retardation effect on the profiles of F_p especially close to the surface. The limiting situations of perfect slip ($\omega = 0$) and no-slip ($\omega = 10000$) at the wall are evident from Fig. 16.

Figures 17 through 20 display the influence of the heat generation (source) or absorption (sink) coefficient ϕ on the profiles of F, F_p, θ, and θ_p, respectively. Obviously, heat generation ($\phi > 0$) causes the temperatures of the fluid phase and the particle phase through interphase heat transfer to increase. This increase in the fluid temperature θ enhances the buoyancy effects for $Gr > 0$ which cause higher induced flow than for the case of $\phi = 0$. Through the interphase drag between the phases, the particle-phase velocity increases as well. Conversely, heat absorption ($\phi < 0$) reduces the temperatures of both phases and, therefore, the velocities of the fluid and particle phases as well for $Gr > 0$. These physical behaviors are clearly depicted in Figs. 17 through 20.

Finally, the effects of the fluid Prandtl number Pr on the profiles of F, F_p, θ, and θ_p are given in Figs. 21 through 24, respectively. Increases in the values of Pr have the tendency to reduce the fluid-phase thermal layer thickness and, therefore, its temperature. As a result, the particle-phase temperature decreases by the action of the interphase heat transfer existing between the phases. As mentioned before, this reduction in the fluid-phase temperature results in fluid-phase flow retardation effect and, therefore, lower particle-phase buoyancy-induced flow by the free convection currents. It is worth noting that for $Pr = 0.71$ distinctive peaks in the velocity profiles of both phases exist at $\eta \cong 1.4$ for which the values of F and F_p overshoot above their free stream values. This is believed to be related to the higher temperature values of both phases predicted for $Pr = 0.71$. These facts are evident from Figs. 21 through 24.

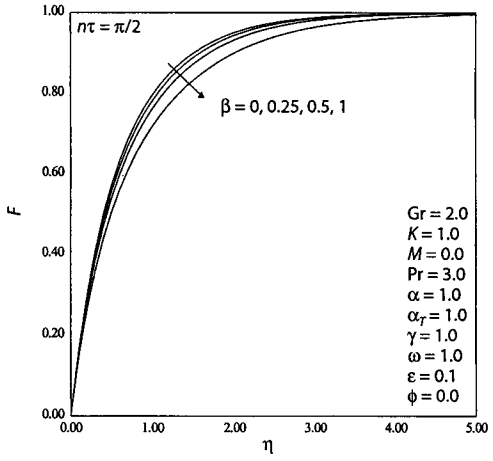

Fig. 13. Effects of β on fluid-phase velocity profiles.

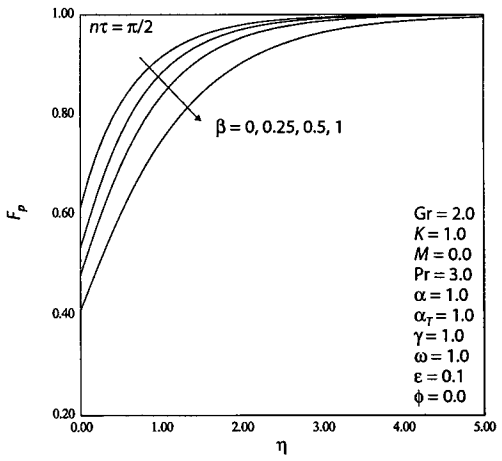

Fig. 14. Effects of β on particle-phase velocity profiles.

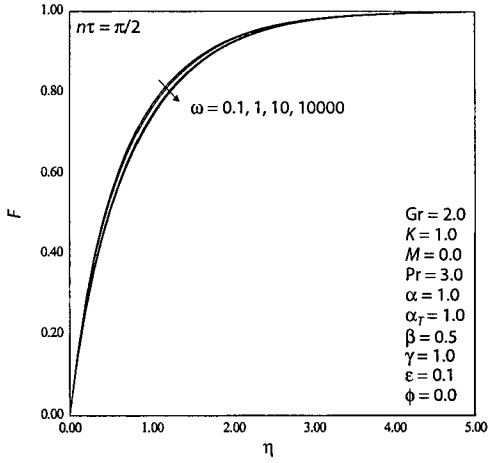

Fig. 15. Effects of ω on fluid-phase velocity profiles.

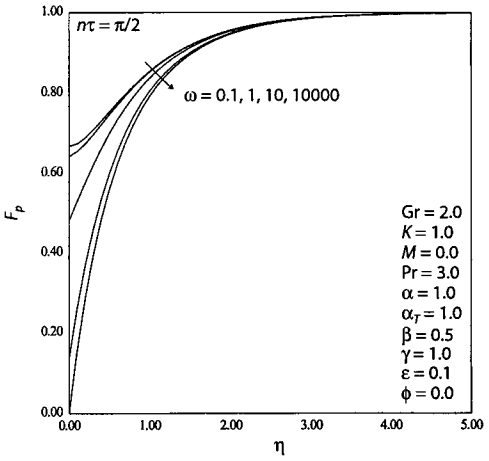

Fig. 16. Effects of ω on particle-phase velocity profiles.

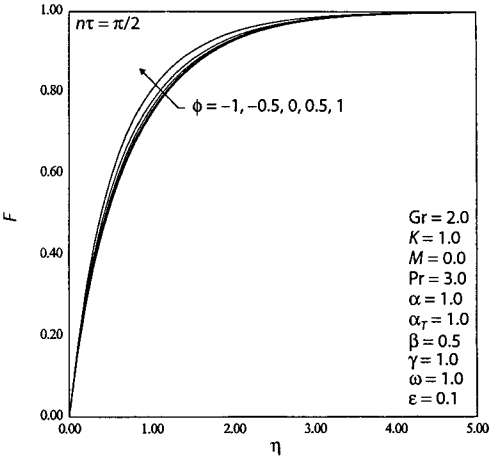

Fig. 17. Effects of φ on fluid-phase velocity profiles.

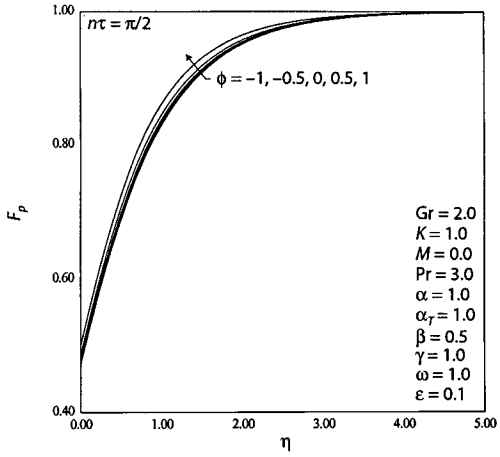

Fig. 18. Effects of φ on particle-phase velocity profiles.

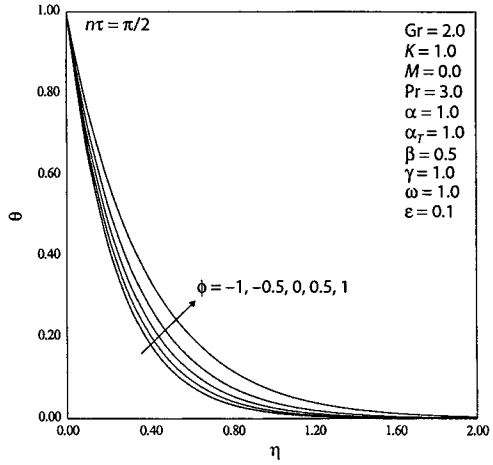

Fig. 19. Effects of φ on fluid-phase temperature profiles.

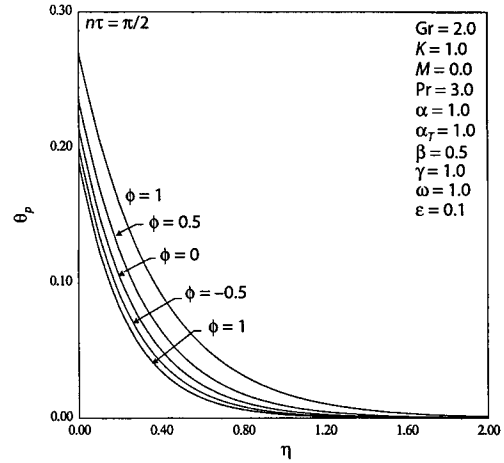

Fig. 20. Effects of φ on particle-phase temperature profiles.

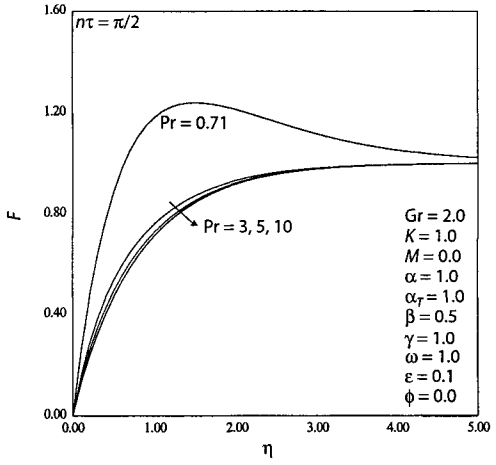

Fig. 21. Effects of Pr on fluid-phase velocity profiles.

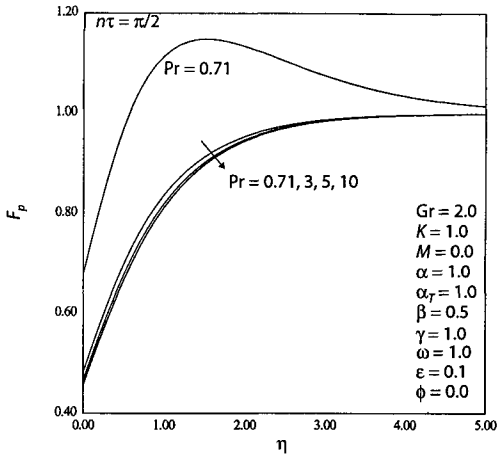

Fig. 22. Effects of Pr on particle-phase velocity profiles.

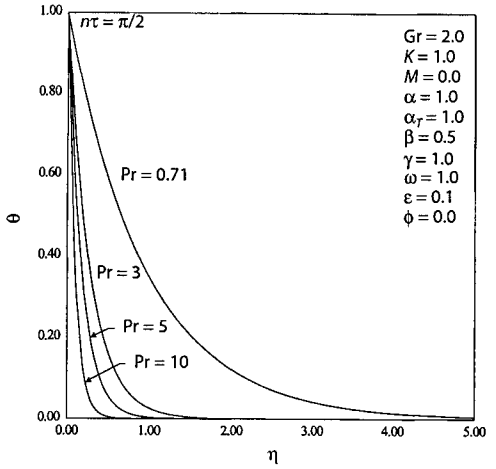

Fig. 23. Effects of Pr on fluid-phase temperature profiles.

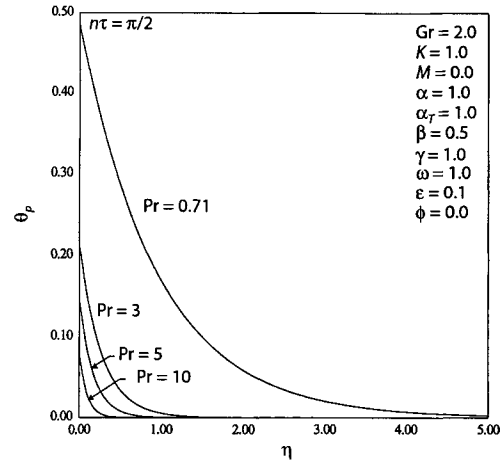

Fig. 24. Effects of Pr on particle-phase temperature profiles.

Summary and Conclusion

The problem of laminar, hydromagnetic, oscillatory natural convection fluid-particle flow over a vertical infinite surface was modeled using a continuum two-phase flow approach. The fluid phase was assumed to be electrically conducting and heat generating or absorbing and the particle phase was assumed to consist of monodispersed spherical particles having a uniform density distribution. The surface was assumed permeable so as to allow for possible wall fluid- and particle-phase suction or blowing and is maintained at a constant temperature. A uniform magnetic field was applied in the direction normal to that of the flow. The free stream velocity of both phases oscillated about a constant mean value. The solid particles and vertical surface were assumed to act as electrical insulators. In addition, the particle-phase was assumed to have an analog pressure and was endowed by a viscosity. Furthermore, the fluid-phase heat generation or absorption effects were assumed to be tempera-

ture-dependent. In the absence of viscous dissipation of both phases, Joule heating, drag-type work, and the Hall effect of magnetohydrodynamics, the derived governing equations were solved analytically for the velocity and temperature profiles of both phases using the regular perturbation technique. The analytical results were compared with previously published work and were found to be in excellent agreement. The effects of the Grashof number, Hartmann number, particle loading, Prandtl number, heat generation or absorption coefficient, viscosity ratio, and the particulate wall slip on the velocity and temperature fields of both phases were illustrated graphically to show interesting features of the solutions. It was found that increasing either of the particle loading, magnetic field strength, Grashof number, or the heat generation or absorption parameter caused the velocities of both phases to increase. On the other hand, increasing either of the viscosity ratio, particle-phase wall slip coefficient, frequency of oscillations or the Prandtl number produced reductions in the velocities of both phases. Moreover, increasing the heat generation or absorption coefficient resulted in increases in the temperature fields of both phases while increasing either of the particle loading or the Prandtl number predicted reductions in both the fluid- and particle-phase temperatures. It is hoped that the results obtained herein be of use for validation of more complex problems dealing with oscillatory two-phase flows.

REFERENCES

1. Hiremath, P. S. and Patil, P. M., Free Convection Effects on the Oscillatory Flow of a Couple Stress Fluid through a Porous Medium, *Acta Mechanica*, 1993, **98**, pp. 143–158.
2. Aldoss, T. K., Al-Nimr, M. A., Jarrah, M. A., and Al-Sha'er, B. J., Magnetohydrodynamic Mixed Convection from a Vertical Plate Embedded in a Porous Medium, *Numerical Heat Transfer, Part A*, 1995, **28**, pp. 635–645.
3. Vajravelu, K. and Hadjinicolaou, A., Heat Transfer in a Viscous Fluid over a Stretching Sheet with Viscous Dissipation and Internal Heat Generation, *Int. Commun. Heat Tranfer*, 1993, **20**, pp. 417–430.
4. Chamkha, A. J. and Ramadan, H., Analytical Solutions for the Two-Phase Free Convection Flow of a Particulate Suspension Past an Infinite Vertical Plate, *Int. J. Eng. Sci.*, 1998, **36**, pp. 49–60.
5. Raptis, A. A. and Perdikis, C. P., Oscillatory Flow through a Porous Medium by the Presence of Free Convective Flow, *Int. J. Eng. Sci.*, 1985, **23**, pp. 51–55.
6. Levesley, J. A., and Bellhouse, B. J., Retention and Suspension of Particles in Fluid Using Oscillatory Flow, *Chemical Engineering Research & Design, Part A: Transactions of the Institute of Chemical Engineers*, 1997, **75**, pp. 288–297.
7. Smith, S. H., Slow Oscillatory Stokes Flow, *Quarterly of Applied Mathematics*, 1997, **55**, pp. 1–22.
8. Hall, K. R., Smith, G. M., and Turcke, D. J., Comparison of Oscillatory and Stationary Flow Through Porous Media, *Coastal Engineering*, 1995, **24**, pp. 217–232.
9. Foote, J. R., Puri, P., and Kythe, P. K., Some Exact Solutions of the Stokes Problem for an Elastico-Viscous Fluid, *Acta Mechanica*, 1987, **68**, pp. 223–230.
10. Soundalgekar, V. M., and Shende, S. R., Oscillatory Flow in a Stratified Medium Past an Infinite Porous Plate with Constant Suction, *Int. J. Energy Research*, 1990, **14**, pp. 53–62.
11. Duck, P. W., and Bodonyi, R. J., Oscillatory Flow over a Semi-Infinite Flat Plate at Low Reynolds Numbers, *Computers & Fluids*, 1988, **16**, pp. 311–326.
12. Mazumdar, B. S. and Das, S. K., Dispersion of Contaminant in Oscillatory Flow through a Pipe. Computation of Moments, *Acta Mechanica*, 1989, **80**, pp. 151–156.